frontiers | Frontiers in Marine Science

TYPE Original Research
PUBLISHED 10 May 2024
DOI 10.3389/fmars.2024.1400798

OPEN ACCESS

EDITED BY
Xianbiao Lin,
Ocean University of China, China

REVIEWED BY
Xiaoli Zhang,
Chinese Academy of Sciences (CAS), China
Shengjie Li,
Max Planck Society, Germany
Matthew Saxton,
Miami University, United States

*CORRESPONDENCE
Yiwen Pan
evelynpan@zju.edu.cn

RECEIVED 14 March 2024
ACCEPTED 29 April 2024
PUBLISHED 10 May 2024

CITATION
Liu Y, Yu L, Yao Z, Shen Y and Pan Y (2024) The effects of turbulence on the growth of three different diatom species. *Front. Mar. Sci.* 11:1400798. doi: 10.3389/fmars.2024.1400798

The effects of turbulence on the growth of three different diatom species

Yijing Liu[1], Lin Yu[1], Zhongzhi Yao[2,3], Yunwen Shen[1] and Yiwen Pan[1]*

[1]Ocean College, Zhejiang University, Zhoushan, China, [2]Ocean Science and Technology College, Hainan Tropical Ocean University, Sanya, China, [3]Yazhou Bay Innovation Institute, Sanya, China

The effects of turbulence on phytoplankton growth have received considerable attentions. However, the complexity of turbulence poses a significant challenge to its systematic characterization in the laboratory, resulting in relatively limited data on the effects of turbulence on several algal species. Here, a laboratory turbulence simulation system was set up to systematically investigate the growth of three common diatom species (*Thalassiosira pseudonana, Skeletonema costatum*, and *Phaeodactylum tricornutum*) under stationary and turbulent conditions (at 60, 120, 180 rpm), and measurements were taken for the algal biomass, algal photosynthetic activity, and nutrients consumption. By comparing the growth of three algae species under different turbulence exposure intensities, this study found that different algae exhibit varying sensitivities to turbulence, and therefore have different shear thresholds. Meanwhile, cell morphology is the key factor influencing the different shear threshold values observed in the three diatom species. Additionally, turbulence could impact algal aggregation and light availability, and dramatically improve nutrient uptake by phytoplankton. Our study will provides theoretical support for future endeavors in using turbulence to cultivate phytoplankton or combat algal blooms.

KEYWORDS

turbulence, phytoplankton, diatom, Thalassiosira pseudonana, Skeletonema costatum, Phaeodactylum tricornutum

1 Introduction

Phytoplankton are common in the ocean and their biological activities could be affected by various environmental factors such as light and temperature, which have been extensively studied (Singh and Singh, 2015). Among these environmental factors, turbulence plays a vital role in numerous processes for phytoplankton, which has both direct and indirect effects (Thorpe, 2005). Directly, it impacts various physiological aspects of phytoplankton, such as cell morphology, antioxidant system, enzyme activities, and photosynthetic activities (Song et al., 2018; Wang and Lan, 2018; Duman et al., 2021).

Indirectly, it affects the growth, reproduction, and activities of phytoplankton by maintaining their suspension in the water column and altering the distribution of nutrients (Peters et al., 2006; Barton et al., 2014), light (Huisman et al., 2004), and water masses.

Diatoms, as a common type of phytoplankton, are diverse and widely distributed, accounting for about 40% of marine primary productivity and playing a significant role in global biogeochemical cycles of carbon and silica (Chrachri et al., 2018; Pujara et al., 2021). They live in the upper layer of oceans and lakes characterized by turbulence (Pujara et al., 2021), and the influence of turbulence on diatoms is intricate and multifaceted, affecting most of the parameters that influence diatom cell survival. It could not only affect settling velocity and re-suspension of diatom cell (Clarson et al., 2009), but also change the velocity of water flow that generate shear stress on the surface of cells, which can cause cell death (Garrison and Tang, 2014).

The impact of turbulence on diatoms species has increasingly become a subject of study, uncovering a multitude of adaptive responses to turbulent stress including nutrients absorption, light utilization, and cell morphology alterations (MaChado et al., 2014; Dell'Aquila et al., 2017). Diatoms, especially the chain forming ones, are considered to optimally thrive in turbulent environments (Dell'Aquila et al., 2017). They are known for their siliceous shells, which confers a certain degree of resistance to the shear stress induced by turbulence. Investigations into the influence of microscale turbulence on the large phytoplankton of a coastal embayment found that formation of siliceous cell chains provide diatoms an advantage in accessing nutrients in turbulent coastal ecosystems (MaChado et al., 2014). Amato et al. studied the morphological response of *Chaetoceros decipiens* to turbulence and suggested that this species produced shorter chains in turbulence (Amato et al., 2017). Additionally, study on the giant diatom *Coscinodiscus* and the small diatom *Thalassiosira pseudonana* demonstrated that the former benefits more from turbulence under phosphorus-limited conditions (Peters et al., 2006). Despite these findings, there is a lack of research on how turbulence affects the growth of various diatom species under the same conditions. In particular, the response of diatoms of various cellular morphologies to turbulence remain poorly understood. Understanding these effects is crucial for elucidating the dynamics of algal populations and their ecological success in natural environments.

Among the common diatoms, *Thalassiosira pseudonana*, *Skeletonema costatum* and *Phaeodactylum tricornutum* exhibit variations in cell morphology (Kröger and Poulsen, 2008). *Thalassiosira pseudonana* can exist alone or as a chain of up to 6 cells, and the central area of the valve surface is usually bounded by an irregular siliceous ring (Belcher and Swale, 1977, 1986). *Skeletonema costatum* is generally a cylindrical chain of 8 to 10 single cells with a thick siliceous shell (Zingone et al., 2005; Michels et al., 2016). *Phaeodactylum tricornutum* exists as single cells of various forms, generally is fusiform, with a few triradiate and oval (Sobczuk et al., 2006). The cytoderm is organic in fusiform and triradiate cells, while it may be organic or one of the valves may have a siliceous shell surrounded by an organic wall in oval cells (Borowitzka and Volcani, 1978). By studying how turbulence affects diatoms with different cell morphologies, researchers can gain a better understanding of the ecological and physiological responses of diatoms to environmental changes.

The complexity of turbulence poses a significant challenge in its systematic characterization within laboratory settings (Peters and Marrasé, 2000). Various methods have been utilized to induce controlled small-scale turbulence in laboratory or enclosed systems, including paddles, oscillating grids, and shakers, which have been extensively used in biological experiments due to their well-developed techniques and adaptability (Sanford, 1997; Amato et al., 2016). Compared to the orbital shaker system, paddles and oscillating grids can generate more spatially consistent, stable, and isotropic small-scale turbulence (Büchs, 2001; Kaku et al., 2006). However, the orbital shaker system is widely used in practical applications due to its simplicity and minimal external interference. Nonetheless, the diverse designs of orbital shakers and the complexities involved in turbulence measurements pose challenges in accurately quantifying turbulence in biological experiments. In many studies, turbulence levels are often estimated through theoretical calculations rather than precise measurements (Peters and Marrasé, 2000). In a previous study, we developed a turbulence simulation system that integrated measuring and simulation methods (Yu et al., 2022). Computational fluid dynamics (CFD) numerical simulations were in good agreement with the experimental results in the measured rotation rates, validating the reliability of our simulation model. This lays the foundation for systematically investigating turbulence's impact on diatoms, which allows us to investigate how turbulence affects various types of diatoms with different cellular morphologies, assisting in distinguishing turbulence effects from other variables such as nutrients, light, and temperature.

Here, we used the orbital shaker system to carry out culture experiments of these three diatoms under different turbulence conditions (0, 60, 120, and 180 rpm). Parameters related to algal growth, including cell density, photosynthetic activities, and nutrients uptake were measured to characterize algal growth. The findings obtained from this study could provide valuable insights into comprehending the impacts of turbulence on the growth of algae.

2 Materials and methods

2.1 Turbulence simulation system

The turbulence simulation system, based on our previous research (Yu et al., 2022), is an orbital oscillator (GUOHUA HY-8) with an orbital diameter of 2.0 cm, as shown in Figure 1. Different turbulence conditions are simulated by setting the rotating rates to 0, 60, 120, and 180 rpm, the oscillation frequencies (f) of which are 1 Hz, 2 Hz, and 3 Hz, respectively.

For each turbulence condition, three identical cylindrical glass serum vials, each measuring 17.5 cm in height, 10 cm in internal diameter, and having a volume of 1 L, were placed on an orbital

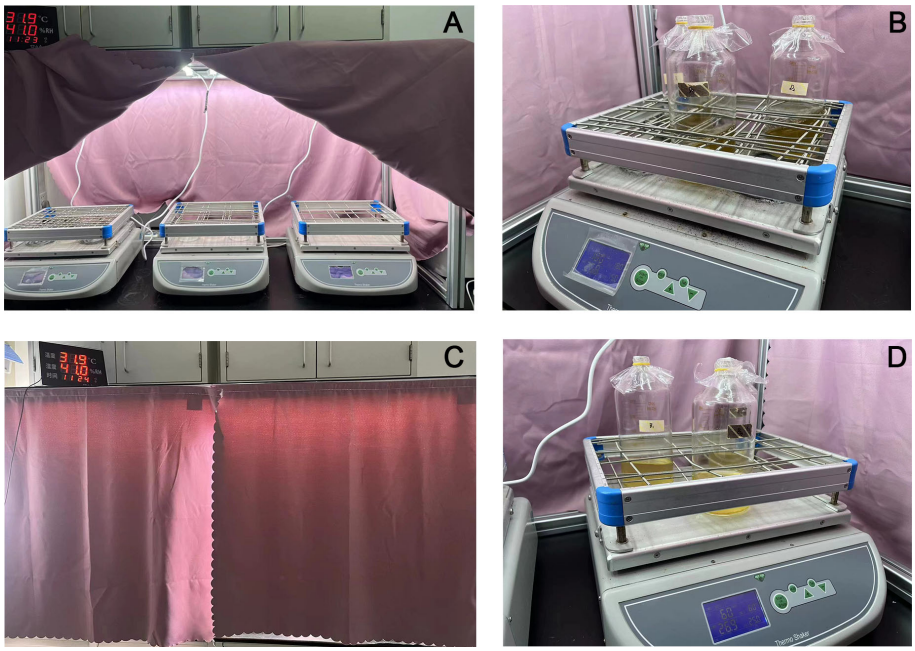

FIGURE 1
Images of the turbulence simulation device: **(A)** the internal structure of the device; **(B, D)** Actual placement of culture reagent bottles; **(C)** the external structure of the device.

oscillator and rotated simultaneously (as shown in Figure 1B). Controlled the light intensity by adjusting the LED light belt above and used a handheld fluorometer (AquaPen 110-C, Photon Systems Instruments, Czech Republic) to determine the light intensity above the bottle to be 2450–2550 lux. A light shield was used to the exterior of the shelf to block any external light sources from the culture system, ensuring that turbulence intensity is the sole experimental variable.

The RANS (Reynolds Averaged Navier-Stokes equations) k-ϵ turbulence model was used to simulate the fluid flow and map the distribution of the turbulent dissipation rate (ϵ) in the orbital oscillation, which has been proved in our previous study (Yu et al., 2022). All parameter settings, including the water level, the temperature and the shape of the container, were the same as those in the experiment.

2.2 Biological culture

2.2.1 Organism and culture conditions

Three marine diatoms, *Phaeodactylum tricornutum*, *Thalassiosira pseudonana*, and *Skeletonema costatum* were cultivated at 25°C with a 12-h light-dark photoperiod cycle, the light intensity of which was about 2450–2550 lux. Equal amounts were transferred into 1 L cylindrical glass serum vials. All experimental equipment was thoroughly cleaned before use. The glassware used was washed with tap water, then soaked in 3 M HCl for 24 h. Afterwards, the glassware was washed with tap water, deionized water and Milli-Q water for three times, then dried in an oven, before being sealed and stored for use. The cells were grown in pre-sterilized and 0.22-μm-filtered artificial seawater enriched with an f/2 medium (Guillard and Ryther, 1962; Guillard, 1975; Berges et al., 2001), the salinity of which is 30.5 psu. The pH of the culture medium was adjusted to 7.6 by adding 1M HCl before sterilization. The experimental diatoms were cultured to the exponential phase before inoculation. Three parallel samples were set under each experimental condition.

2.2.2 Physiological parameters determination

A sample of 100 mL of algae solution was obtained from each experimental set and was used for further testing. The growth of experimental algae was described by daily cell counts. 1 mL of the culture medium was removed from the conical flask to a 2 mL microcentrifuge tube and then fixed in Lugol's iodine solution for later detailed analysis (Kim et al., 2017). 0.1 mL of samples was pipetted into a 0.1 mL volume counting plate, and was left for 30 minutes to allow the cells to settle. The counting plate has 100 identical chambers, each with a volume of 1 μL. Five chambers were randomly selected under a light microscope (CX-43, OLYMPUS, Japan) and the number of cells in each chamber was counted and averaged to represent the number of cells in 1μL. From this the algal cell density is calculated. The maximum photochemical quantum yield (Fv/Fm) was determined by Hand-held algae fluorimeter. 6 mL of algal liquid was filtered by 0.22 μm glass fiber membrane to determine the nitrate (NO_3^-).

2.3 Statistical analysis

Three parallel samples were set under each experimental condition. All of the results are expressed as mean values with the standard deviation. Statistical analysis of the experimental data was

conducted using SPSS statistical software (SPSS Statistics 22.0, IBM, Armonk, NY, USA). We first subjected the data for each group to the KolmogorovSmirnov test to verify that they were normally distributed ($p > 0.05$). Then, to estimate the effect of investigated factors on the analyzed parameters, multifactorial analysis of variance (ANOVA, San Francisco, CA, USA) was applied combined with Tukey's multiple comparison tests, where statistical significance was set at a 0.05 level.

3 Results

3.1 Turbulence simulation

The water level in the serum vials was set as 12.5 cm during simulation. Figure 2 illustrates the simulated flow field in the container at rotating rate of 60, 120, and 180 rpm, providing an accurate representation of the experimental setup under real conditions. The results show the distribution of the turbulence dissipation rates (ϵ) within the container, encompassing both the liquid and gas phases.

The turbulent flow distribution within the liquid exhibits a nearly symmetrical pattern, with the axis of symmetry aligned along the centerline of the cylindrical serum bottle (Figures 2A–C). As the distance from the liquid surface decreases, the fluctuations intensify, resulting in greater turbulence dissipation rates, higher turbulence intensity and a denser distribution of energy gradients. Due to the boundary effect, both ϵ and its gradient increase with decreasing distance from the side and bottom walls. Another difference in turbulent field distribution occurs in the serum bottles. For example, the minimum value of ϵ is observed in the region close to the wall at 60 rpm, in the center of the lower part of the vessel at 120 rpm, and in the center of the entire liquid fraction at 180 rpm.

From the ϵ distribution, although the ϵ range at 60 rpm, 120 rpm, and 180 rpm on the liquid surface is wide, spanning from 10^{-7} to 10^{-4} m^2 s^{-3} (Figures 2A–C) the corresponding distribution characteristics of algae shown in Figures 2E–G indicate that algae were not uniformly distributed within the culture medium. For instance, at 60 rpm, the overall turbulent field distribution remains predominantly in the range of 10^{-7} to 10^{-6}, with the turbulent field below the liquid surface being dominant. Most algae grow in the lower 1/3 of the culture medium, and algae aggregates can be observed at the bottom, indicating that algae mainly inhabit a turbulent field with ϵ of approximately 10^{-7} to 10^{-6} m^2 s^{-3}. At 120 rpm and 180 rpm, although the magnitude of ϵ changes more dramatically, reaching 10^{-7} to 10^{-5} and 10^{-6} to 10^{-4} m^2 s^{-3}, respectively. At 120 rpm, algae mainly inhabit the lower 1/2 of the culture medium, with trace amounts of algae still aggregating at the bottom, indicating that most algae live in an environment with ϵ ranging from 10^{-6} to 10^{-5} m^2 s^{-3}. At 180 rpm, the color of the culture medium noticeably darkens, and no algae aggregates are observed at the bottom. Algae are thus more evenly dispersed throughout the entire water body, indicating that they inhabit an environment with ϵ ranging from 10^{-6} to 10^{-4} m^2 s^{-3}. Consequently, this turbulence simulation system can simulate ϵ of appropriate intensity, which can be applied to the study of the effect of turbulence on algae.

To characterize the turbulence generated in the cylindrical container, we established the section coordinate system of the

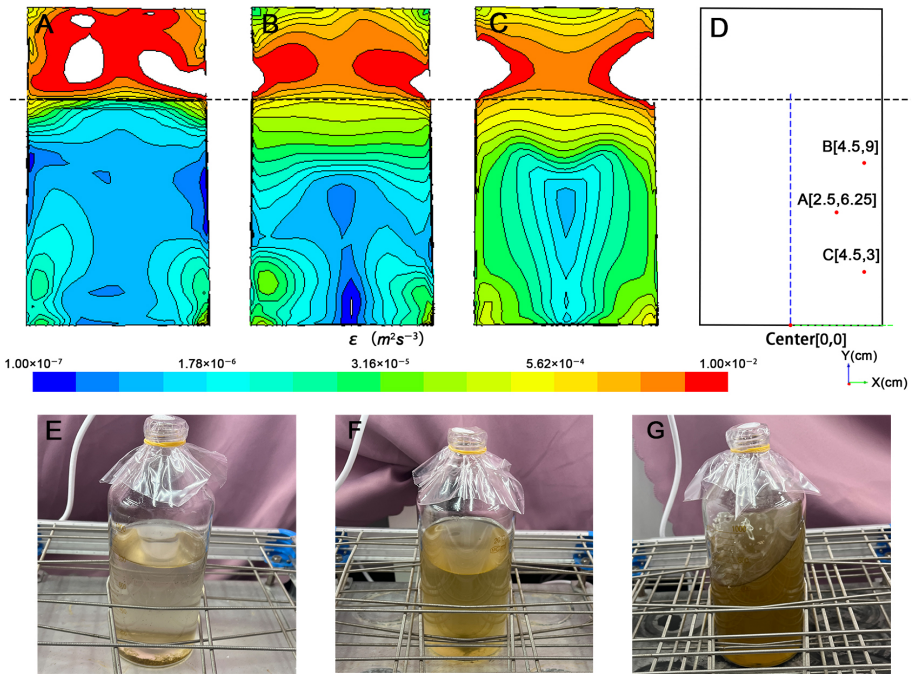

FIGURE 2
The CFD model of the culture system at the rotation rates of **(A)** 60 rpm, **(B)** 120 rpm, **(C)** 180 rpm, **(D)** is the coordinate system of the flask established with the center of the bottle bottom as the origin, the algae distribution of **(E)** 60 rpm, **(F)** 120 rpm, **(G)** 180 rpm.

container with the center of bottle bottom as the origin, the radius x, and the vertical bottom surface as y based on the premise that the distribution of the turbulent field in the container is basically axisymmetric (Figure 2D). In order to better characterize the real turbulent environment in which algae live, three sites (A, B, and C) was selected to represent the situation of the liquid part in the container and the corresponding ϵ and scale were calculated. Different turbulence intensities correspond to different length scale, including the Kolmogorov length scale for the smallest eddy (η), and the Batchelor length scale for stirring (η_b) (Jumars et al., 2009; Taylor and Stocker, 2012). The turbulence dissipation rate (ϵ) data and corresponding length scale are shown in Table 1. According to the results, the ϵ of 60 rpm is the smallest and its corresponding length scale is the largest at both A and B, while at C, the ϵ of 120 rpm is the smallest and its length scale is the largest. The maximum ϵ of the three points appear at A and C at 180 rpm and at B at 120 rpm, respectively. Taking A, B, and C as characteristic points to represent the overall level of turbulent field in the container, it can be found that the ϵ of 60 rpm is less than that of 120 rpm, which involves a wide range but still less than 180 rpm. It is worth noting that in all three cases, η_b is much smaller than η, and the order of η is basically 10^2 to 10^3, while η_b is only 10, which is similar to the size of the microalgae used in the experiment. In the realistic marine environment, η usually ranges from 300 to 1000 µm and is usually 2000 µm in the mixed layer of seawater surface, which is generally considered to affect only the growth of large phytoplankton or cell colonies, but has little effect on microalgae (Barton et al., 2014). η_b is much smaller than η, ranging from 10 to 250 µm which is similar to our calculation. This size matches most small phytoplankton and turbulence could therefore affect the nutrient absorption of smaller phytoplankton (Guasto et al., 2012; Barton et al., 2014). η and η_b generated by the turbulence simulation system used in this study are within the range of the marine environment, and the difference in intensity is controllable, which indicates the reliability of this turbulence simulation system to study the effects of small-scale turbulence on phytoplankton and community, especially for plankton with relatively limited mobility and small volume.

3.2 The response of microalgae under different turbulence conditions

To better understand the growth of *Thalassiosira pseudonana, Skeletonema costatum*, and *Phaeodactylum tricornutum*, this study conducted systematic monitoring of the entire process for each of these algae. Typical plots of cell density, maximum photochemical quantum yield (Fv/Fm), and NO_3^- were presented in Figure 3. Typical plots of cell density, maximum photochemical quantum yield (Fv/Fm), and NO_3^- as a proportion of control group (stationary group) were presented in Figure 4. In the culture, all algae rapidly entered exponential growth periods under various turbulence conditions.

3.2.1 Response of *Thalassiosira pseudonana* under turbulence

For *Thalassiosira pseudonana*, biomass increased from the original $2.73 \pm 0.43 \times 10^5$ to the $33.45 \pm 1.44 \times 10^5$ cell/mL, from $2.84 \pm 0.03 \times 10^5$ to $46.43 \pm 3.75 \times 10^5$ cell/mL, from $2.24 \pm 0.03 \times 10^5$ to $46.73 \pm 1.33 \times 10^5$ cell/mL, and from $2.26 \pm 0.29 \times 10^5$ to $57.53 \pm 2.53 \times 10^5$ cell/mL for 0, 60, 120, and 180 rpm conditions, respectively (Figure 3A). The growth rates in all groups slowed down on day 6. During the first two days culture, there was no significant difference (Table S1) in the growth rates of *Thalassiosira pseudonana* between the stationary group and the turbulent group (60 rpm). At 180 rpm turbulence, a slightly lower growth rate was observed, indicating the need for adaptation at 180 rpm turbulence. Subsequently, the cell density of algae in the three turbulent exposure groups began to exceed that of the stationary group and was significantly higher at the end of the cultivation period. Among the three speeds, there was no significant difference ($p > 0.05$) in algae growth rates between the 60 rpm and 120 rpm groups, while the 180 rpm group showed a significantly higher growth rate than the others. The maximum photochemical quantum yield (Fv/Fm) is a characterization of the photosynthetic efficiency of algae. As shown in Figure 3B, Fv/Fm of *Thalassiosira pseudonana* in the four sets increased in the first two days and then began to decline.

TABLE 1 Individual turbulence parameters for sites A, B, and C within the flask.

Sites	Rotating rates	0 rpm	60 rpm	120 rpm	180 rpm
	Frequencies (Hz)	0	1	2	3
A	ϵ (m^2s^{-3})	—	5.5×10^{-7}	7.9×10^{-7}	9.0×10^{-6}
	η (µm)	—	1160	1062	578
	η_b (µm)	—	37	34	18
B	ϵ (m^2s^{-3})	—	3.4×10^{-7}	1.2×10^{-5}	7.3×10^{-5}
	η (µm)	—	1309	537	343
	η_b (µm)	—	41	17	11
C	ϵ (m^2s^{-3})	—	7.6×10^{-6}	1.0×10^{-6}	3.9×10^{-5}
	η (µm)	—	602	990	401
	η_b (µm)	—	19	31	13

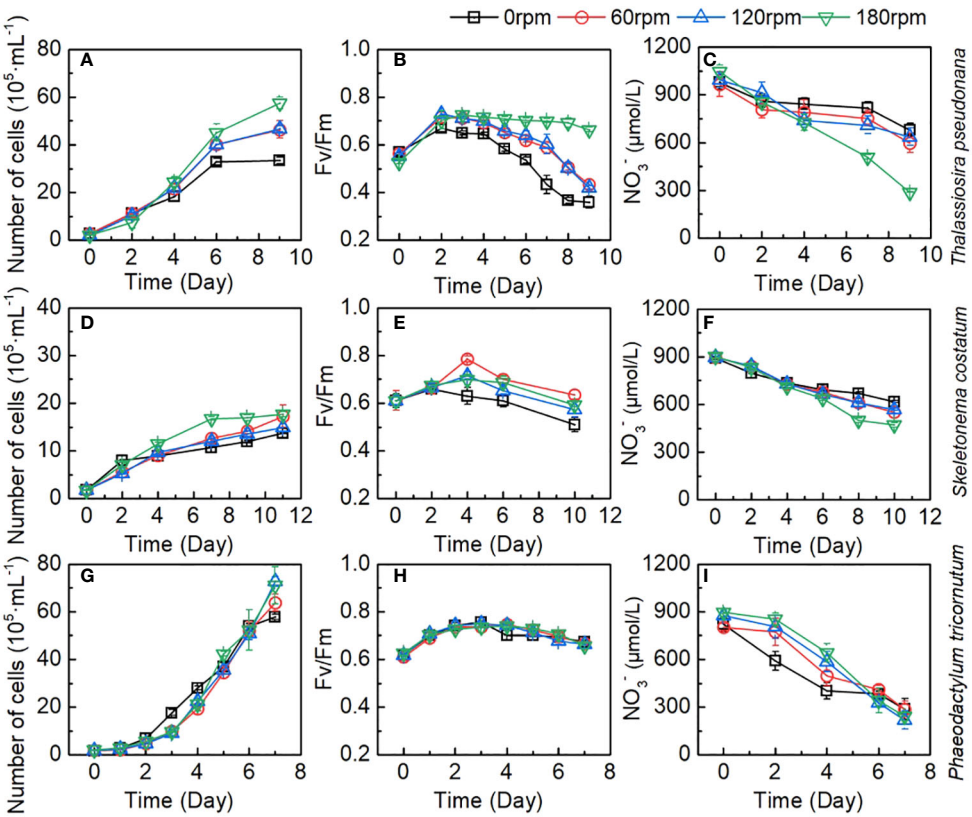

FIGURE 3
Changes of number of cells, Fv/Fm, and NO_3^- during the culture of **(A–C)** *Thalassiosira pseudonana*; **(D–F)** *Skeletonema costatum*; **(G–I)** *Phaeodactylum tricornutum* under different turbulence intensities. Each point is the mean of three replicate incubations and error bars represent the standard deviation of replicates (n=3).

All groups exhibited the highest Fv/Fm values on the second day, with the turbulent cultivation groups having higher values than the stationary group thereafter (Figure 3B). With the increase in turbulence, the declining trend of Fv/Fm in all groups showed that the stationary group had the fastest decline, experiencing a rapid decline after the fourth day and slowing down by the eighth day. In the 60 rpm and 120 rpm groups, especially the 60 rpm group, a faster decline rate was observed on the fourth day, but a noticeable rapid decline occurred on the seventh day. In the 180 rpm group, a significant decline in Fv/Fm was observed only on the eighth day. The changes of NO_3^- in the medium during the algae growth were shown in Figure 3C. In the initial two days, there was no significant difference in NO_3^- consumption between the stationary group and the turbulent groups. However, after the second day, with the increase in turbulence intensity and algae density, NO_3^- consumption also increased. At the end of the cultivation period, the NO_3^- in the 180 rpm group decreased to 291.1 ± 2.1 μmol/L, which is significantly lower than the other three groups.

Therefore, the growth rates, Fv/Fm, and NO_3^- consumption among different groups reflect that the growth status of algae in the high-rotation group is superior to that in the low-rotation group, and superior to the stationary group. This suggests that turbulence stimulated the growth of *Thalassiosira pseudonana*.

Even at a rotation speed of 180 rpm, the shear forces generated by turbulence have not reached the threshold to inhibit its growth, demonstrating the strong tolerance of *Thalassiosira pseudonana* to the damaging effects of turbulence. Interestingly, the increase in rotation speed did not uniformly enhance the growth capacity of *Thalassiosira pseudonana*. Take the Fv/Fm values as an example, Fv/Fm values were very close between the 60 rpm and 120 rpm groups, with a significant improvement observed in the 180 rpm group. This phenomenon is also evident in the changes in algae growth rates and NO_3^-, suggesting that the increased turbulence in the 180 rpm group may bring about other factors that promote the algal growth. Considering the turbulence dissipation rate, there was a significant increase at 180 rpm, and we speculate that this may be related to the matching of the Batchelor length with the size of the algae, making it easier for the algae to access nutrients. Additionally, we observed that in the 180 rpm group, algae were evenly distributed throughout the culture bottle, whereas in the stationary, 60 rpm, and 120 rpm groups, algae mainly inhabited the lower half of the culture bottle (Figures 2E–G). Hence, the significant improvement in the 180 rpm group may be due to reducing the shading effect of algae, thereby enhancing light utilization, leading to a prominent increase in the growth and reproduction of *Thalassiosira pseudonana* in this group. Therefore, the increased growth of algae in the 180 rpm group

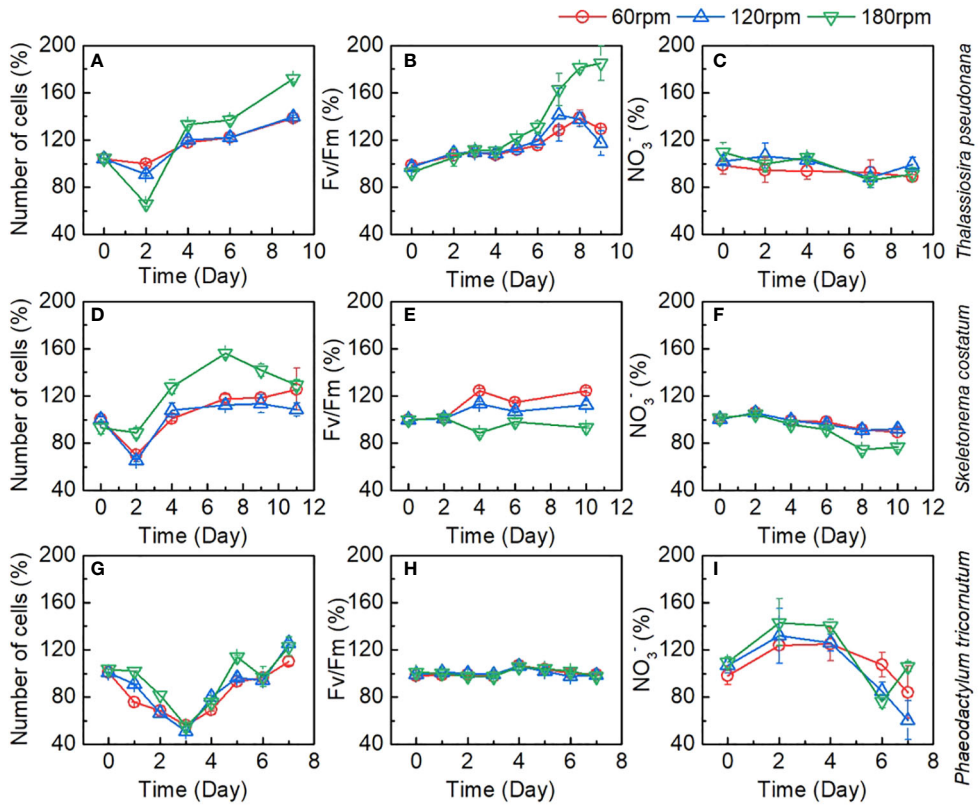

FIGURE 4
Changes of number of cells, Fv/Fm, and NO_3^- as a proportion of control group during the culture of **(A–C)** *Thalassiosira pseudonana*; **(D–F)** *Skeletonema costatum*; **(G–I)** *Phaeodactylum tricornutum* under different turbulence intensities. Each point is the mean of three replicate incubations and error bars represent the standard deviation of replicates (n=3).

could be attributed to an increase in the availability of light or a more efficient distribution of nutrients within the bottle.

3.2.2 Response of *Skeletonema costatum* under turbulence

For *Skeletonema costatum*, the growth rates, Fv/Fm, and NO_3^- consumption among different groups were shown in Figures 3D–F. A period of exponential growth was observed in all four groups during 11 days of cultivation. The number of algal cells increased from the initial 1.80 ± 0.04 × 10^5 to the final 16.12 ± 0.51 × 10^5 cell/mL, from 1.80 ± 0.01 × 10^5 to 21.76 ± 0.72 × 10^5 cell/mL, from 1.80 ± 0.05 × 10^5 to 19.40 ± 0.21 × 10^5 cell/mL, and from 1.68 ± 0.07 × 10^5 to 18.11 ± 0.47 × 10^5 cell/mL for 0, 60, 120, and 180 rpm, respectively. The stationary group exhibited the fastest growth rate in the first two days, followed by a significant decline in growth rate thereafter. In the turbulent groups, except for the 180 rpm group, the algae growth rates under 60 rpm and 120 rpm cultivation showed a significant reduction compared to the stationary group in the first four days, and slightly decreased after four days. However, due to the substantial decrease in growth rate in the stationary group after two days, the algae growth rates in the 60 rpm and 120 rpm groups surpassed the stationary group after the fourth day and remained consistently higher thereafter. Between 60 rpm and 120 rpm, the growth curves were very close, with no significant difference observed in the first nine days. Since we continued the cultivation of *Skeletonema costatum* until the 11th day and found that from the 11th day onward, the growth rate of *Skeletonema costatum* in the 120 rpm group was lower than that in the 60 rpm group (Figure 4E). In the 180 rpm group, the algae exhibited a different growth pattern from the other turbulent groups. It maintained a growth rate similar to the stationary state in the first four days. However, after that, the growth rate abruptly dropped to very low levels, and for the next four days, the algae density remained constant at approximately 17 × 10^5 cell/mL. Similar phenomena can be seen in Fv/Fm and NO_3^-. As shown in Figure 3E, Fv/Fm in the stationary group began to decline after increasing for the first two days, while Fv/Fm in the turbulent group continued to increase until day 4 and remained higher than that in the stationary group until the end of the cultivation. After day 4, 60 rpm group and 120 rpm group existed a similar rate of decline, both of which first decreased sharply and then slowed down, but the values of the 60 rpm group were always higher than those of the 120 rpm group. The 180 rpm group maintained a downward trend similar to that of the stationary group after day 4, declined slowly from day 4 to day 6, after which the rate of decline increased slightly, with a value between that of the 60 rpm group and that of the stationary group. Figure 3F shows the change of NO_3^- under different turbulence intensities. The stationary group had the

highest NO_3^- consumption rate for the first two days, and there was no significant difference in NO_3^- consumption between three turbulent groups in the initial two days. After the second day, the NO_3^- consumption rate of the stationary group became lower than that of the turbulent group at 60 rpm and 120 rpm. The NO_3^- consumption rate of 60 rpm and 120 rpm groups is very close during the cultivation. In the 180 rpm group, NO_3^- consumption rate is higher than that in the other groups on day 4 and shows a trend of slowing down on day 8. However, it is worth noting that NO_3^- consumption rate did not slow down significantly in relation to the growth rate, and that a slight increase in the NO_3^- consumption rate was then observed.

Consequently, the growth rates, Fv/Fm, and NO_3^- consumption among different groups generally reflected the stimulating effect of turbulence on *Skeletonema costatum* growth. Interestingly, more obvious differences caused by different turbulence intensity were detected during day 2–7, suggesting that the effect of turbulence on algal growth was cumulative over time. In 180 rpm group, both the growth rate and NO_3^- consumption rate were significantly reduced after day 8, indicating the effect of continuous turbulent action on algal growth.

3.2.3 Response of *Phaeodactylum tricornutum* under turbulence

For *Phaeodactylum tricornutum*, in contrast to *Thalassiosira pseudonana* and *Skeletonema costatum*, all cultures exposed to different turbulence conditions exhibited similar growth curves. This distinct growth pattern of *Phaeodactylum tricornutum*, diverging from the other two diatom groups, may be attributed to its robust reproductive capacity and the absence of a silica shell. Within the initial four days, the growth curves under turbulence entirely overlapped and continued to intermingle until the conclusion of day 7. In the stationary group, algae exhibited faster growth compared to the turbulent groups from day 2 to day 5, after which growth rates became similar, with a slight decrease observed on day 7. The lack of a silica shell in *Phaeodactylum tricornutum* resulted in a significantly higher initial growth rate in the stationary group than in the turbulent exposure groups, which also led to a decrease in the proportion of turbulent groups to control group (Figure 4G). By the fourth day, the cell density in the stationary group reached 3×10^6 cell/mL, indicating a high algal density that may have limited further growth. This phenomenon is also reflected in the Fv/Fm parameter (Figure 3H). Fv/Fm values showed no significant difference between the stationary group and the three turbulent groups during the first three days. However, a significant decrease in Fv/Fm was observed in the stationary group on day 4 and 5, which may have been caused by growth factor limitation induced by the high algae density. The variation in NO_3^- in the culture medium during the growth process, as shown in Figure 3I, generally mirrored the growth rate of algae. The NO_3^- consumption rate was significantly higher in the stationary group during the first 4 days, followed by a significant slowdown until day 7, when NO_3^- remained relatively consistent across all groups.

Therefore, the growth rate, Fv/Fm and NO_3^- consumption among different groups reflect that turbulence has no significant effect on *Phaeodactylum tricornutum*. Compared with *Thalassiosira pseudonana* and *Skeletonema costatum*, the differences among the four sets of *Phaeodactylum tricornutum* are relatively small, which may be related to its robust reproductive capacity, overriding the impact of turbulence.

4 Discussion

In the marine ecosystems, the ϵ ranges from 10^{-10} to 10^{-2} m^2 s^{-3} (Yamazaki and Osborn, 1988), although ϵ above 10^{-2} m^2 s^{-3} are mainly found in areas affected by storms and frontal systems (Guadayol and Peters, 2006; Guadayol et al., 2009). In estuarine and coastal regions with gale conditions, or the ϵ is higher in straight lowland rivers, which can reach about 10^{-6} to 10^{-3} m^2 s^{-3} (Sukhodolov et al., 1998). Compared with the turbulence intensity existing in the ocean, the maximum turbulence intensity generated by the turbulence simulation system used in our study reaches a higher level in the range (Figure 2). However, in laboratory settings, it is common to create conditions with higher turbulence intensity than those found in natural environments. Bardalet et al. also used an orbital shaker to conduct a relatively high intensity of ϵ (bulk average: 2.01×10^{-4} m^2 s^{-3}, range: 2.7×10^{-5} to 2.4×10^{-3} m^2 s^{-3}) (Berdalet et al., 2007). This is done to aid in elucidating the potential mechanisms by which planktonic organisms adapt to turbulence. By measuring the growth parameters of three species of diatoms under different turbulence intensities, it was observed that the turbulence simulation system used in this study generally promoted algae growth, leading to higher cell density and nutrients consumption. However, the response to varying turbulence intensity differed among the three types of algae, reflecting the influence of turbulence on environmental conditions and algal cells.

In the stationary group, growth inhibition after rapid growth of algae was seen in all cultured algae, but the time of occurrence was not the same. *Thalassiosira pseudonana* appeared on day 6, *Skeletonema costatum* on day 2, and *Phaeodactylum tricornutum* on day 4 (Figure 3). This phenomenon should be due to the fact that after algae density reaches a certain threshold, the factors required for algae growth in environmental conditions are inhibited. Such factors may be the availability of light and nutrients (Barton et al., 2014), resulting in the inhibition of algae growth, and its main feature is the rapid reduction of Fv/Fm values seen in the previous few days.

In turbulent groups, changes were very similar for the 60 rpm and 120 rpm groups, but less so for the 180 rpm group (Figure 3). For *Thalassiosira pseudonana*, growth inhibition occurred in both the 60 rpm and 120 rpm groups at the later stages of cultivation, as evidenced by a slowdown in growth rate and a decrease in Fv/Fm. However, the stronger turbulence (180 rpm) still favored its growth, as shown by significantly higher cell number, Fv/Fm and NO_3^- uptake than the other groups. For *Skeletonema costatum*, the continuous effect of the excessively strong turbulence (180 rpm) apparently produced a significant inhibition of their growth, as shown by a sharp drop in growth rate on day 7. For *Phaeodactylum tricornutum*, there was no significant difference in the response to different intensities of turbulence. This phenomenon is thought to

be a superposition of the different morphologies of the three diatoms, as well as different environmental conditions such as light availability and shear force caused by different turbulence intensities.

4.1 Nutrients availability

Figure 5 shows the NO_3^- reduction of the three diatoms every two days under different turbulence intensities, revealing distinct responses of the algae to nutrient uptake under different turbulence intensities. In the stationary groups, the amount of NO_3^- absorbed by the three kinds of algae showed a gradually decreasing trend during day 2–6, which is likely related to the low NO_3^- concentration in the vicinity of algal cells. The much higher ΔNO_3^- in *Phaeodactylum tricornutum* indicates its greater ability to capture nutrients, corresponding well with its strong reproductive capacity. After day 6, an increase in ΔNO_3^- was observed, which could be caused by algal cell death and subsequent remineralization. For the turbulent groups, the presence of the turbulence significantly inhibited the NO_3^- absorption of *Phaeodactylum tricornutum* and *Skeletonema costatum* in the first two days, while only *Thalassiosira pseudonana* showed a slight promotion under 60 rpm conditions. This suggests that *Phaeodactylum tricornutum* and *Skeletonema costatum* have an adaptation period to turbulence at the current turbulence intensity, while *Thalassiosira pseudonana* appears to be highly resistant to turbulence.

After an adaptation period, the three algae species exhibit a characteristic where turbulence promotes the cell density and nutrient concentration consumption. Barton et al. suggested that diffusion-limited resource concentration boundary layers would be formed when the nutrient concentration reduced at the cell surface drops below that of the bulk medium during nutrient uptake, which is generally much larger than the cells themselves (Barton et al., 2014). These boundary layers act as constraints on the ability of algae to acquire high nutrient concentrations, particularly for non-motile species. This phenomenon may provide insight into the differential occurrence of dinoflagellate and diatom blooms, with tranquil waters favoring dinoflagellate blooms, while diatom blooms are more common after disturbances (Huisman et al., 2004; Clarson et al., 2009). Turbulence-induced distortion of these boundary layer alters nutrient gradients (Pasciak and Gavis, 1974) and the movement of algae with the liquid enhances nutrient circulation within algal cells, facilitating material exchange (Blersch et al., 2013; Huang et al., 2016). Consequently, turbulence improves the ability of algal cells to absorb nutrients from the medium.

Comparing the calculated η_b values in this experiment, it is evident that η_b decreases as turbulence intensity increase. However, the reduction in η_b does not scale proportionally with the increase in rotational speed (Table 1). When the rotating rate increase from 60 rpm to 120 rpm, the average difference in η_b at three feature

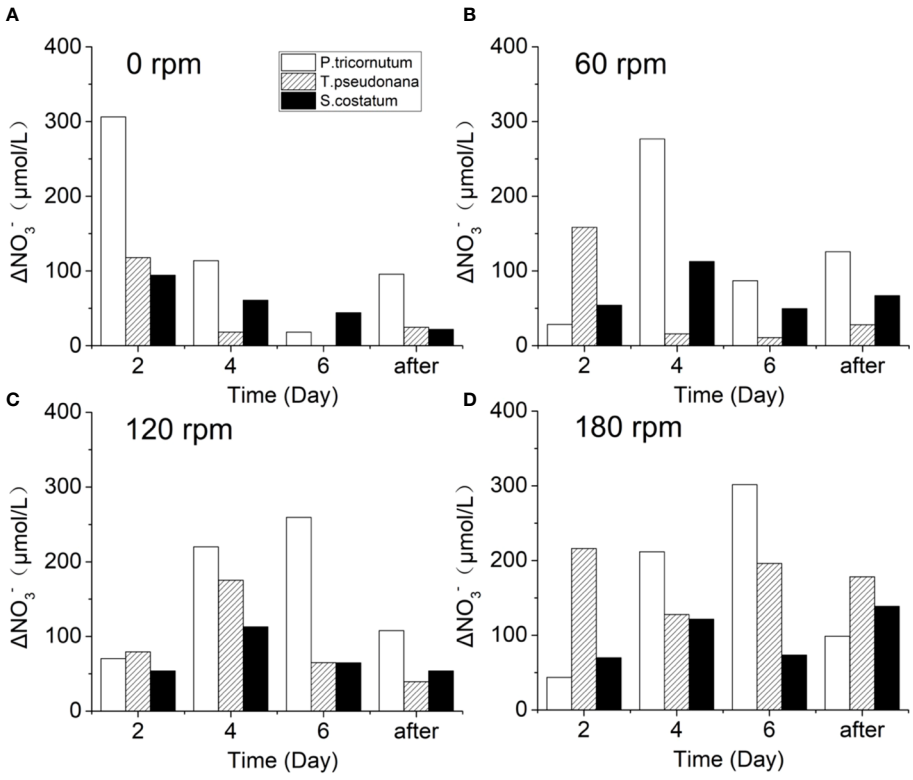

FIGURE 5
Changes of ΔNO_3^- during the culture of three diatoms under turbulence intensity of **(A)** 0 rpm, **(B)** 60 rpm, **(C)** 120 rpm, and **(D)** 180 rpm.

points is not particularly significant, with minimum values of 19 μm and 17 μm, and the rest ranging from 37–41 μm and 31–34 μm respectively. However, when the rotating rate was 180 rpm, the η_b at the three characteristic points was only 11–18 μm.

The size of the three diatoms in this experiment varied: the individual cell diameters of *Thalassiosira pseudonana* was 4–5 μm, and *Thalassiosira pseudonana* was mostly observed as individual cells in this study; the individual cell diameters of *Skeletonema costatum* were 5–6 μm, forming chains of around 10 cells, with a size of approximately 40 μm; the individual cell diameters of *Phaeodactylum tricornutum* was 9–10 μm.

The analysis of *Thalassiosira pseudonana* reveals intriguing insights into its response to varying turbulence intensities. With individual sizes ranging from 4–5 μm in non-chain formation, *Thalassiosira pseudonana* reaches a size approaching η_b only at 180 rpm. In terms of nutrient acquisition, no adaptation period is observed as turbulence intensity increases from stationary conditions to 60 rpm, indicating a significant increase in nutrients uptake capacity (Figures 5A, B). This indicates that *Thalassiosira pseudonana* exhibits a strong tolerance to turbulence. As the turbulence intensity increases from 60 rpm to 120 rpm, a short adaptation period emerges, indicating a suppressing effect on *Thalassiosira pseudonana* (Figures 5B, C). The slight increase in the maximum amplitude of ΔNO_3^- from 60 rpm to 120 rpm, aligns with the negligible enhancement in nutrient acquisition capacity, as reflected by the change in η_b. Under the 180 rpm condition (Figure 5D), it is surprisingly found that the maximum value of ΔNO_3^- reappears on day 2, and the adaptation period observed at 120 rpm disappears under the 180 rpm condition, underscoring *Thalassiosira pseudonana*'s robust tolerance to turbulence. This suggests that when turbulence intensity reaches a certain threshold and algae size approaches η_b, the promoting effect on nutrient uptake becomes pronounced. Additionally, under the 180 rpm condition, the intense turbulent oscillations lead to a more uniform distribution of cells, increased living space, and improved lighting conditions, favoring its growth (Figure 2G). Therefore, this may indicate that the turbulence tolerance threshold of algae species with higher turbulence tolerance may be correlated with other environmental factors.

For *Phaeodactylum tricornutum*, which has a size of 9–10 μm, slightly bigger than *Thalassiosira pseudonana*. The η_b values at both 60 rpm and 120 rpm are slightly smaller than the size of *Phaeodactylum tricornutum*, while at 180 rpm, the η_b matches its size. Therefore, the nutrients uptake capacity of *Phaeodactylum tricornutum* should significantly increase at 180 rpm. However, the ΔNO_3^- did not show a significant increase at 180 rpm (Figure 5D). Additionally, no apparent differences in cell density and Fv/Fm under different turbulence conditions were observed (Figures 3G, H). This could be due to *Phaeodactylum tricornutum*'s superior growth ability, enabling it to adequately acquire nutrients for its growth even at stationary state. In previous studies, *Phaeodactylum tricornutum* has been demonstrated to be a good competitor for nutrients (D'Elia et al., 1979; Zhao et al., 2015). Or it could be that under high turbulence conditions, a large number of algae die due to the lack of a silica shell protection, resulting in the inability to demonstrate an increase in nutrient uptake by algae.

For *Skeletonema costatum, the* η_b at 60 rpm matches its cell size, effectively addressing nutrient uptake issues. Consequently, from 60 rpm to 120 rpm, *Skeletonema costatum* did not exhibit a significant increase in nutrient uptake and the growth rate of the 60 rpm group remained even faster (Figures 4B, C). Although the increase in environmental factors such as living space and light at 180 rpm condition may also contribute to the enhanced NO_3^- absorption capacity of the algae, the magnitude of this increase is limited.

4.2 Shear stress

The impact of turbulence on algal growth exhibits a dual nature, where appropriate turbulence intensity can promote growth, but excessively high intensity can damage algal cells and inhibit reproduction due to strong shear forces. Nutrient data indicates that all three algae species experience an adaptation period from the stationary state to under turbulence. Furthermore, the duration of this adaptation period increases with the intensity of turbulence. However, it is noteworthy that the timing and duration of the adaptation period vary among different algal species.

Among them, *Thalassiosira pseudonana* exhibits the strongest turbulence tolerance. Except for the phenomenon of needing adaptation in the absorption rate of NO_3^- under 120 rpm turbulence intensity, even when the turbulence dissipation rate increases (to 180 rpm condition), the growth rate, Fv/Fm values, and nutrient absorption rate do not seem to reach its turbulence tolerance threshold (Figures 3A–C). This indicates that the shear stress has not reached the limit for cell damage in *Thalassiosira pseudonana*, hence *Thalassiosira pseudonana* shows a continuous improvement in growth status with increasing turbulence intensity.

For *Skeletonema costatum*, the assistance of turbulence intensity in nutrient uptake remains generally consistent after 60 rpm. The Fv/Fm values and the plateauing of cell density in the late stages of cultivation at 180 rpm suggest that the shear stress reaches the turbulence tolerance threshold of *Skeletonema costatum* during the transition from 120 rpm to 180 rpm. Similar phenomena was reported by Michels et al. who found that *Skeletonema costatum* was not impacted by shear stress at 1.2 Pa. However, when the shear stress was increased from 5.4 Pa to 25 Pa, the survival rate of *Skeletonema costatum* decreased from 80.5% to 73.4% (Michels et al., 2016). Furthermore, the growth rate of *Skeletonema costatum* decreased significantly at the late stage of culture under the continuous action of turbulence in the 180 rpm condition suggests that for *Skeletonema costatum*, a chain-forming diatom with a siliceous shell, the impact of turbulence on its growth appears to have a cumulative time-dependent effect. Similar accumulative effects were observed in the study by Juhl et al. on *lingulodinium polyedrum*. They found that the relative growth inhibition caused by oscillations in the late exponential growth stage was greater than that in the early stage (Juhl et al., 2000).

For *Phaeodactylum tricornutum*, shear forces exert the greatest damage to algal cells in our experiment. The growth rate of *Phaeodactylum tricornutum* in the stationary state is significantly faster than that in turbulent conditions. At turbulence intensities of 60 rpm, 120 rpm, and 180 rpm (corresponding to ϵ range from

5.5×10^{-7} m^2 s^{-3} to 7.3×10^{-5} m^2 s^{-3}), the algal density and the Fv/Fm are almost completely intertwined. This suggests that *Phaeodactylum tricornutum* seems to have poor resistance to turbulence, as even relatively weak turbulence intensities are adequate to rupture some algal cells. Consequently, despite *Phaeodactylum tricornutum*'s robust growth capability, its cell density remains mixed together under various turbulence intensities. Miron et al. suggested that as the rate of the surface bubble increased from 0.01m/s to 0.02m/s during *Phaeodactylum tricornutum* cultivation, the biomass change from stable to decrease, indicating the damaging effect of turbulence caused by air bubbles on algal cells (Mirón et al., 2003). For similar algae lacking siliceous shell protection, there are reports of cell disruption phenomena as well. Camacho et al. observed that *Protoceratium reticulatum* experienced sudden cell disruption when grown in a shake-flask with a shear stress level of 1.6×10^{-4} Pa, despite the growth being similar to static culture for the first 5 days. This demonstrates the adverse effect of cumulative shear stress (Rodríguez et al., 2009). Additionally, *Protoceratium reticulatum* cells grown at low shear stress and then exposed to high shear forces were more sensitive than those originally grown at high shear stress, leading to faster cell death when exposed to high shear stress levels. Hence, algal growth is affected not only by the applied shear stress but also by the duration and proportion of time exposed to it. Different combinations of duration and cycle frequency result in different critical shear stresses.

4.3 Cell morphology

It was observed in our study that both the enhancement of nutrient utilization capacity by turbulence and the inhibitory effect of shear forces on algae exhibit notable species dependence. These promoting or inhibitory effects seem to correlate with the variations in morphology among the three diatom species.

Chain diatoms like *Skeletonema costatum* are considered to be the most suitable for living in turbulent environment. There are large gaps between the cells that could lead to the assumption that water could flow through these gaps. Under turbulence, the total nutrient supply per cell can become much greater for cells in a chain with gaps than for solitary cells due to the impact of chain length on advection, thus promoting its growth (Pasciak and Gavis, 1974; Pahlow et al., 1997; Maar et al., 2002; Peters et al., 2006; Musielak et al., 2009). However, if the intensity of turbulence is too extreme, the chain will break (Sherman et al., 1998; Clarson et al., 2009; Hondzo and Wüest, 2009; Dell'Aquila et al., 2017). *Thalassiosira pseudonana* could exist alone or as a chain of up to 6 cells, and the central area of the valve surface is usually bounded by an irregular siliceous ring (Belcher and Swale, 1977, 1986). *Skeletonema costatum* is generally a cylindrical chain of 8 to 10 single cells with a thick siliceous shell (Zingone et al., 2005; Michels et al., 2016). As Figure 6 shown, *Thalassiosira pseudonana* exists as a single cell and *Skeletonema costatum* exist as a chain in this study. The siliceous cell walls of *Thalassiosira pseudonana* and *Skeletonema costatum* could help them resist the shear force from outside (Kröger and Poulsen, 2008), enabling them to adapt and survive more easily in turbulent environments (Smayda, 1997). However, due to the length of the *Skeletonema costatum*'s chain, it is more susceptible to break under the action of high-intensity turbulence. According to the result from Michels et al., longer chains of *Skeletonema costatum* disappeared after 1 day with more short chains and single cells as a result, and broken and disintegrated cells were seen after a few days. This may have led to differences in their ability to adapt to turbulence. For

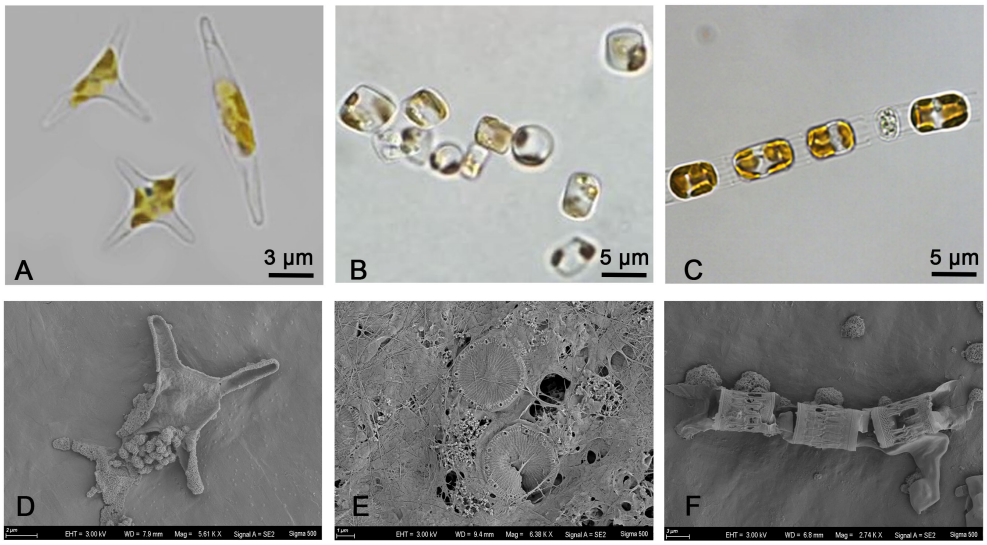

FIGURE 6
Optical microscope image of **(A)** Phaeodactylum tricornutum, **(B)** Thalassiosira pseudonana, **(C)** Skeletonema costatum. Scanning electron microscope (SEM) image of **(D)** Phaeodactylum tricornutum, **(E)** Thalassiosira pseudonana, **(F)** Skeletonema costatum.

Phaeodactylum tricornutum, it exists as single cells of fusiform or triradiate forms in this study. Its cell wall is completely organic without a silica skeleton that lacks the ability to resist shear forces (Borowitzka and Volcani, 1978; Sobczuk et al., 2006). Besides, its reproductive capacity is strong, and the combination of two factors may lead to its lack of obvious response to turbulence. Thus, different turbulence intensities have different effects on different algal species due to different cell morphology, depending on their cell structure and chain length.

5 Conclusions

Building upon previous studies, this study combines experimental and simulation approaches to further establish a turbulence simulation system suitable for practical laboratory applications. The study focuses on investigating the specific effects of three different diatom species (*Thalassiosira pseudonana, Skeletonema costatum*, and *Phaeodactylum tricornutum*) under static conditions and three different turbulent conditions, including algal density, photosynthetic activity, and nutrient uptake. The distribution of the turbulence field in the culture flasks was analyzed by software simulation, and characteristic turbulence parameters were calculated and compared with those in natural environments, demonstrating reliability of the turbulence simulation system in generating relatively uniform small-scale turbulence in laboratory. By measuring the growth of three diatoms under different turbulence exposure intensities, it was observed that the turbulence simulation system used in our study generally promoted algae growth, leading to higher cell density and nutrient consumption compared with static water conditions. Meanwhile, different algal species exhibit varying sensitivities to turbulence, which may be related to nutrient availability, sustained shear action and cell morphology. These results summarized the effects of turbulence on algal growth, and will provide guidance for future efforts in utilizing turbulence to cultivate microalgae or combat algal blooms. In future, experiments should be carried out to investigate specific turbulence intensity thresholds for typical algae to provide more detailed data.

Data availability statement

The original contributions presented in the study are included in the article/Supplementary Material. Further inquiries can be directed to the corresponding author.

Author contributions

YL: Data curation, Formal Analysis, Investigation, Methodology, Validation, Writing – original draft. LY: Data curation, Formal Analysis, Investigation, Methodology, Validation, Writing – original draft. ZY: Formal Analysis, Visualization, Writing – original draft. YS: Formal Analysis, Writing – original draft. YP: Data curation, Funding acquisition, Writing – original draft, Writing – review & editing.

Funding

The author(s) declare that financial support was received for the research, authorship, and/or publication of this article. This work was supported by the National Natural Science Foundation of China (Grant No. 42176036), the Major Project of Basic Public Welfare Research Program of Zhejiang Province (Grant No. LD24D060002), the Major Industrial Science and Technology Research Project of Zhoushan City (Grant No. 2023C03003), the Assessment of Blue Carbon Stocks and Blue Carbon Sinking Potential of Zhoushan Island Group Ecosystem (Grant DH-2022ZY0006), Hainan Provincial Natural Science Foundation of Chinas (Grant No. 422MS081), and the Ocean Negative Carbon Emission (ONCE) program.

Acknowledgments

The authors would be thankful to Prof. Weiqi Fu for providing the test platform, Prof. Mengmeng Tong for identifying algae species from sea samples, and the laboratory technician Yuxia Sun for the help in nitrate measurements.

Conflict of interest

The authors declare that the research was conducted in the absence of any commercial or financial relationships that could be construed as a potential conflict of interest.

Publisher's note

Supplementary material

The Supplementary Material for this article can be found online at: https://www.frontiersin.org/articles/10.3389/fmars.2024.1400798/full#supplementary-material

References

Amato, A., Dell'Aquila, G., Musacchia, F., Annunziata, R., Ugarte, A., Maillet, N., et al. (2017). Marine diatoms change their gene expression profile when exposed to microscale turbulence under nutrient replete conditions. *Sci. Rep.* 7, 3826. doi: 10.1038/s41598–017-03741–6

Amato, A., Fortini, S., Watteaux, R., Diano, M., Espa, S., Esposito, S., et al. (2016). TURBOGEN: Computer-controlled vertically oscillating grid system for small-scale turbulence studies on plankton. *Rev. Sci. Instrum.* 87, 035119. doi: 10.1063/1.4944813

Barton, A. D., Ward, B. A., Williams, R. G., and Follows, M. J. (2014). The impact of fine-scale turbulence on phytoplankton community structure: Phytoplankton and turbulence. *Limnol. Oceanogr.* 4, 34–49. doi: 10.1215/21573689-2651533

Belcher, J. H., and Swale, E. M. F. (1977). Species of *Thalassiosira* (Diatoms, Bacillariophyceae) in the plankton of English rivers. *Br. Phycol. J.* 12, 291–296. doi: 10.1080/00071617700650311

Belcher, J. H., and Swale, E. M. F. (1986). Notes on some small *Thalassiosira* species (Bacillariophyceae) from the plankton of the lower thames and other British Estuaries (identified by transmission electron microscopy). *Br. Phycol. J.* 21, 139–145. doi: 10.1080/00071618600650161

Berdalet, E., Peters, F., Koumandou, V. L., Roldán, C., Guadayol, Ò., and Estrada, M. (2007). Species-specific physiological response of dinoflagellates to quantified small-scale turbulence [1]. *J. Phycol.* 43, 965–977. doi: 10.1111/j.1529-8817.2007.00392.x

Berges, J. A., Franklin, D. J., and Harrison, P. J. (2001). Evolution of an artificial seawater medium: improvements in enriched seawater, artificial water over the last two decades. *J. Phycol.* 37, 1138–1145. doi: 10.1046/j.1529-8817.2001.01052.x

Blersch, D. M., Kangas, P. C., and Mulbry, W. W. (2013). Turbulence and nutrient interactions that control benthic algal production in an engineered cultivation raceway. *Algal. Res.* 2, 107–112. doi: 10.1016/j.algal.2013.01.001

Borowitzka, M. A., and Volcani, B. E. (1978). The polymorphic diatom *Phaeodactylum tricornutum*: Ultrastructure of its morphotypes. *J. Phycol.* 14, 10–21. doi: 10.1111/j.1529-8817.1978.tb00625.x

Büchs, J. (2001). Introduction to advantages and problems of shaken cultures. *Biochem. Eng. J.* 7, 91–98. doi: 10.1016/S1369-703X(00)00106-6

Chrachri, A., Hopkinson, B. M., Flynn, K., Brownlee, C., and Wheeler, G. L. (2018). Dynamic changes in carbonate chemistry in the microenvironment around single marine phytoplankton cells. *Nat. Commun.* 9, 74. doi: 10.1038/s41467-017-02426-y

Clarson, S. J., Steinitz-Kannan, M., Patwardhan, S. V., Kannan, R., Hartig, R., Schloesser, L., et al. (2009). Some observations of diatoms under turbulence. *Silicon* 1, 79–90. doi: 10.1007/s12633-009-9018-y

D'Elia, C. F., Guillard, R. R. L., and Nelson, D. M. (1979). Growth and competition of the marine diatoms *Phaeodactylum tricornutum* and *Thalassiosira pseudonana* I. Nutrient effects. *Mar. Biol.* 50, 305–312. doi: 10.1007/BF00387007

Dell'Aquila, G., Ferrante, M. I., Gherardi, M., Cosentino Lagomarsino, M., Ribera d'Alcalà, M., Iudicone, D., et al. (2017). Nutrient consumption and chain tuning in diatoms exposed to storm-like turbulence. *Sci. Rep.* 7, 1828. doi: 10.1038/s41598–017-02084–6

Duman, E. T., Kose, A., Celik, Y., and Oncel, S. S. (2021). Design of a horizontal-dual bladed bioreactor for low shear stress to improve hydrodynamic responses in cell cultures: A pilot study in *Chlamydomonas reinhardtii*. *Biochem. Eng. J.* 169, 107970. doi: 10.1016/j.bej.2021.107970

Garrison, H. S., and Tang, K. W. (2014). Effects of episodic turbulence on diatom mortality and physiology, with a protocol for the use of Evans Blue stain for live–dead determinations. *Hydrobiologia* 738, 155–170. doi: 10.1007/s10750-014-1927-0

Guadayol, Ò., Marrasé, C., Peters, F., Berdalet, E., Roldán, C., and Sabata, A. (2009). Responses of coastal osmotrophic planktonic communities to simulated events of turbulence and nutrient load throughout a year. *J. Plankton Res.* 31, 583–600. doi: 10.1093/plankt/fbp019

Guadayol, Ò., and Peters, F. (2006). Analysis of wind events in a coastal area: a tool for assessing turbulence variability for studies on plankton. *Sci. Mar.* 70, 9–20. doi: 10.3989/scimar.2006.70n19

Guasto, J. S., Rusconi, R., and Stocker, R. (2012). Fluid mechanics of planktonic microorganisms. *Annu. Rev. Fluid Mech.* 44, 373–400. doi: 10.1146/annurev-fluid-120710-101156

Guillard, R. R. L. (1975). "Culture of phytoplankton for feeding marine invertebrates," in *Culture of Marine Invertebrate Animals*. Eds. W. L. Smith and M. H. Chanley (Springer US, Boston, MA), 29–60. doi: 10.1007/978–1-4615–8714-9_3

Guillard, R. R. L., and Ryther, J. H. (1962). Studies of marine planktonic diatoms: I. Cyclotella Nana Hustedt, and Detonula confervacea (Cleve) gran. *Can. J. Microbiol.* 8, 229–239. doi: 10.1139/m62-029

Hondzo, M., and Wüest, A. (2009). Do microscopic organisms feel turbulent flows? *Environ. Sci. Technol.* 43, 764–768. doi: 10.1021/es801655p

Huang, J., Xi, B., Xu, Q., Wang, X., Li, W., He, L., et al. (2016). Experiment study of the effects of hydrodynamic disturbance on the interaction between the cyanobacterial growth and the nutrients. *J. Hydrodyn.* 28, 411–422. doi: 10.1016/S1001-6058(16)60644-3

Huisman, J., Sharples, J., Stroom, J. M., Visser, P. M., Kardinaal, W. E. A., Verspagen, J. M. H., et al. (2004). Changes in turbulent mixing shift competition for light between phytoplankton species. *Ecology* 85, 2960–2970. doi: 10.1890/03-0763

Juhl, A. R., Velazquez, V., and Latz, M. I. (2000). Effect of growth conditions on flow-induced inhibition of population growth of a red-tide dinoflagellate. *Limnol. Oceanogr.* 45, 905–915. doi: 10.4319/lo.2000.45.4.0905

Jumars, P. A., Trowbridge, J. H., Boss, E., and Karp-Boss, L. (2009). Turbulence-plankton interactions: a new cartoon. *Mar. Ecol.* 30, 133–150. doi: 10.1111/j.1439-0485.2009.00288.x

Kaku, V. J., Boufadel, M. C., and Venosa, A. D. (2006). Evaluation of mixing energy in laboratory flasks used for dispersant effectiveness testing. *J. Environ. Eng.* 132, 93–101. doi: 10.1061/(ASCE)0733-9372(2006)132:1(93)

Kim, H., Bok, T.-H., Paeng, D.-G., Kim, J., Nam, K.-H., Lee, J.-B., et al. (2017). Mobility of *Amphidinium carterae* Hulburt measured by high-frequency ultrasound. *J. Acoust. Soc. America* 141, EL395–EL401. doi: 10.1121/1.4980007

Kröger, N., and Poulsen, N. (2008). Diatoms—from cell wall biogenesis to nanotechnology. *Annu. Rev. Genet.* 42, 83–107. doi: 10.1146/annurev.genet.41.110306.130109

Maar, M., Arin, L., Simó, R., Sala, M., Peters, F., and Marrasé, C. (2002). Combined effects of nutrients and small-scale turbulence in a microcosm experiment. II. Dynamics of organic matter and phosphorus. *Aquat. Microb. Ecol.* 29, 63–72. doi: 10.3354/ame029063

MaChado, D. A., Marti, C. L., and Imberger, J. (2014). Influence of microscale turbulence on the phytoplankton of a temperate coastal embayment, Western Australia. *Estuar. Coast. Shelf Sci.* 145, 80–95. doi: 10.1016/j.ecss.2014.04.018

Michels, M. H. A., van der Goot, A. J., Vermuë, M. H., and Wijffels, R. H. (2016). Cultivation of shear stress sensitive and tolerant microalgal species in a tubular photobioreactor equipped with a centrifugal pump. *J. Appl. Phycol.* 28, 53–62. doi: 10.1007/s10811-015-0559-8

Mirón, A. S., García, M. C. C., Gómez, A. C., Camacho, F. G., Grima, E. M., and Chisti, Y. (2003). Shear stress tolerance and biochemical characterization of *Phaeodactylum tricornutum* in quasi steady-state continuous culture in outdoor photobioreactors. *Biochem. Eng. J.* 16, 287–297. doi: 10.1016/S1369-703X(03)00072-X

Musielak, M. M., Karp-Boss, L., Jumars, P. A., and Fauci, L. J. (2009). Nutrient transport and acquisition by diatom chains in a moving fluid. *J. Fluid Mech.* 638, 401–421. doi: 10.1017/S0022112009991108

Pahlow, M., Riebesell, U., and Wolf-Gladrow, D. A. (1997). Impact of cell shape and chain formation on nutrient acquisition by marine diatoms. *Limnol. Oceanogr.* 42, 1660–1672. doi: 10.4319/lo.1997.42.8.1660

Pasciak, W. J., and Gavis, J. (1974). Transport limitation of nutrient uptake in phytoplankton: Transport limitation of uptake. *Limnol. Oceanogr.* 19, 881–888. doi: 10.4319/lo.1974.19.6.0881

Peters, F., Arin, L., Marrasé, C., Berdalet, E., and Sala, M. M. (2006). Effects of small-scale turbulence on the growth of two diatoms of different size in a phosphorus-limited medium. *J. Mar. Syst.* 61, 134–148. doi: 10.1016/j.jmarsys.2005.11.012

Peters, F., and Marrasé, C. (2000). Effects of turbulence on plankton: an overview of experimental evidence and some theoretical considerations. *Mar. Ecol. Prog. Ser.* 205, 291–306. doi: 10.3354/meps205291

Pujara, N., Du Clos, K. T., Ayres, S., Variano, E. A., and Karp-Boss, L. (2021). Measurements of trajectories and spatial distributions of diatoms (Coscinodiscus spp.) at dissipation scales of turbulence. *Exp. Fluids* 62, 149. doi: 10.1007/s00348–021-03240–5

Rodríguez, J. J. G., Mirón, A. S., Camacho, F. G., García, M. C. C., Belarbi, E. H., Chisti, Y., et al. (2009). Causes of shear sensitivity of the toxic dinoflagellate *Protoceratium reticulatum*. *Biotechnol. Prog.* 25, 792–800. doi: 10.1002/btpr.161

Sanford, L. (1997). Turbulent mixing in experimental ecosystem studies. *Mar. Ecol. Prog. Ser.* 161, 265–293. doi: 10.3354/meps161265

Sherman, B. S., Webster, I. T., Jones, G. J., and Oliver, R. L. (1998). Transitions between *Auhcoseira* and *Anabaena* dominance in a turbid river weir pool. *Limnol. Oceanogr.* 43, 1902–1915. doi: 10.4319/lo.1998.43.8.1902

Singh, S. P., and Singh, P. (2015). Effect of temperature and light on the growth of algae species: A review. *Renewable Sustain. Energy Rev.* 50, 431–444. doi: 10.1016/j.rser.2015.05.024

Smayda, T. J. (1997). Harmful algal blooms: Their ecophysiology and general relevance to phytoplankton blooms in the sea. *Limnol. Oceanogr.* 42, 1137–1153. doi: 10.4319/lo.1997.42.5_part_2.1137

Sobczuk, T. M., Camacho, F. G., Grima, E. M., and Chisti, Y. (2006). Effects of agitation on the microalgae *Phaeodactylum tricornutum* and *Porphyridium cruentum*. *Bioprocess Biosyst. Eng.* 28, 243–250. doi: 10.1007/s00449-005-0030-3

Song, Y., Zhang, L.-L., Li, J., Chen, M., and Zhang, Y.-W. (2018). Mechanism of the influence of hydrodynamics on *Microcystis aeruginosa*, a dominant bloom species in reservoirs. *Sci. Total Environ.* 636, 230–239. doi: 10.1016/j.scitotenv.2018.04.257

Sukhodolov, A., Thiele, M., and Bungartz, H. (1998). Turbulence structure in a river reach with sand bed. *Water Resour. Res.* 34, 1317–1334. doi: 10.1029/98WR00269

Taylor, J. R., and Stocker, R. (2012). Trade-offs of chemotactic foraging in turbulent water. *Science* 338, 675–679. doi: 10.1126/science.1219417

Thorpe, S. A. (2005). *The turbulent ocean* (Cambridge; New York: Cambridge University Press).

Wang, C., and Lan, C. Q. (2018). Effects of shear stress on microalgae – A review. *Biotechnol. Adv.* 36, 986–1002. doi: 10.1016/j.biotechadv.2018.03.001

Yamazaki, H., and Osborn, T. R. (1988). "Review of oceanic turbulence: implications for biodynamics," in *Toward a Theory on Biological-Physical Interactions in the World Ocean*. Ed. B. J. Rothschild (Springer Netherlands, Dordrecht), 215–234. doi: 10.1007/978–94-009–3023-0_12

Yu, L., Li, Y., Yao, Z., You, L., Jiang, Z.-P., Fan, W., et al. (2022). Characterization of fine-scale turbulence generated in a laboratory orbital shaker and its influence on *Skeletonema costatum*. *JMSE* 10, 1053. doi: 10.3390/jmse10081053

Zhao, Y., Wang, Y., and Quigg, A. (2015). Comparison of population growth and photosynthetic apparatus changes in response to different nutrient status in a diatom and a coccolithophore. *J. Phycol.* 51, 872–884. doi: 10.1111/jpy.12327

Zingone, A., Percopo, I., Sims, P. A., and Sarno, D. (2005). Diversity in the genus *Skeletonema* (Bacillariophyceae). I. A reexamination of the type material of s.*Costatum* with the description of s. *Grevillei* sp. *J. Phycol.* 41, 140–150. doi: 10.1111/j.1529-8817.2005.04066.x